Laser-driven collimated tens-GeV monoenergetic protons from mass-limited target plus preformed channel

F. L. Zheng, S. Z. Wu, H. C. Wu, C. T. Zhou, H. B. Cai, M. Y. Yu, T. Tajima, X. Q. Yan, and X. T. He

Citation: Physics of Plasmas (1994-present) **20**, 013107 (2013); doi: 10.1063/1.4775728
View online: http://dx.doi.org/10.1063/1.4775728
View Table of Contents: http://scitation.aip.org/content/aip/journal/pop/20/1?ver=pdfcov
Published by the AIP Publishing

Laser-driven collimated tens-GeV monoenergetic protons from mass-limited target plus preformed channel

F. L. Zheng,[1] S. Z. Wu,[1,2] H. C. Wu,[1] C. T. Zhou,[1,2] H. B. Cai,[1,2] M. Y. Yu,[3,4] T. Tajima,[5] X. Q. Yan,[1,6,a)] and X. T. He[1,2,b)]
[1]*Key Laboratory of HEDP of the Ministry of Education, CAPT, Peking University, Beijing 100871, China*
[2]*Institute of Applied Physics and Computational Mathematics, Beijing 100088, China*
[3]*Institute of Fusion Theory and Simulation, Zhejiang University, Hangzhou 310027, China*
[4]*Institut für Theoretische Physik I, Ruhr-Universität Bochum, D-44780 Bochum, Germany*
[5]*Fakultät f. Physik, LMU München, Garching D-85748, Germany,*
[6]*State Key Laboratory of Nuclear Physics and Technology, Peking University, Beijing 100871, China*

(Received 10 September 2012; accepted 27 December 2012; published online 11 January 2013)

Proton acceleration by ultra-intense laser pulse irradiating a target with cross-section smaller than the laser spot size and connected to a parabolic density channel is investigated. The target splits the laser into two parallel propagating parts, which snowplow the back-side plasma electrons along their paths, creating two adjacent parallel wakes and an intense return current in the gap between them. The radiation-pressure pre-accelerated target protons trapped in the wake fields now undergo acceleration as well as collimation by the quasistatic wake electrostatic and magnetic fields. Particle-in-cell simulations show that stable long-distance acceleration can be realized, and a 30 fs monoenergetic ion beam of >10 GeV peak energy and <2° divergence can be produced by a circularly polarized laser pulse at an intensity of about 10^{22} W/cm^2. © *2013 American Institute of Physics*. [http://dx.doi.org/10.1063/1.4775728]

I. INTRODUCTION

Laser-driven ion acceleration has been of much recent interest because of its broad scientific and technical applications. Protons with tens to hundreds MeV energies are useful for cancer therapy,[1] fast ignition in inertial confinement fusion,[2] high resolution radiography,[3–8] laser nuclear physics,[9] etc. Ions with still higher energies are relevant to high energy physics research.[10]

Radiation pressure acceleration (RPA) is promising for obtaining high-quality ion beams efficiently.[11–13] Existing studies have shown that GeV proton beams can be obtained by RPA using circularly polarized (CP) lasers with intensity above 10^{22} W/cm^2.[14–16] However, because of transverse instabilities and hole-boring by the laser pulse,[14–17] the acceleration length is rather limited and it is difficult to enhance proton energy without still higher laser intensity. Recently, it has been shown that tens GeV proton beams[18,19] can be obtained by sequential radiation pressure and bubble acceleration or a moving double-layer, or in a two-phase acceleration regime[20,21] by ultra-relativistic lasers. However, in classical RPA and laser wakefield acceleration (LWFA),[22] the accelerated ion bunch tends to diverge because of the ubiquitous intense space-charge field.[23–25] The resulting defocusing leads to rather low ion flux. Moreover, the effective laser-plasma interaction distance is also limited by laser diffraction. As a result, ions cannot remain collimated and be accelerated stably over a long distance.

In this paper, we propose a stable proton acceleration scheme using an ultra-intense CP laser pulse and a mass-limited target (MLT)[26] connected to an underdense parabolic plasma channel. The target splits the laser pulse into two separate but adjacent parts, which are then refractively guided by the preformed underdense plasma channel. The quasistatic longitudinal accelerating and transverse collimating fields associated with the electron return current at the center of the channel can then stably trap, collimate, and further accelerate the RPA target protons by LWFA over a long distance. In contrast to the existing acceleration schemes, both proton defocusing and laser diffraction do not occur here. Particle-in-cell (PIC) simulations show that ultrashort (30 fs) monoenergetic proton beams with peak energy >10 GeV and divergence angle less than 2° can be obtained with a $\sim 10^{22}$ W/cm^2 CP laser pulse.

II. PRODUCING HIGHLY COLLIMATED TENS-GeV MONOENERGETIC PROTONS IN THE TWIN-WAKES REGIME

A. PIC simulation modeling

To demonstrate the proposed scheme, we use the two-dimensional (2D) PIC code KLAP.[27] The CP laser pulse is of wavelength $\lambda = 1\,\mu$m and peak intensity $I_0 = 9.8 \times 10^{21}$ W/cm^2 (or the normalized laser parameter $a_0 = 60$). It has a super-Gaussian radial profile with spot size $2\sigma = 40\lambda$ and a $18\,T$ flattop envelope, where T is the laser period. The fully ionized uniform hydrogen MLT of thickness $D = 0.8\lambda$ and density of $N = 20n_c$, where n_c is the critical density, is initially located in $50\lambda \le x \le 50.8\lambda$, $-10\lambda \le y \le 10\lambda$. Behind the hydrogen MLT is an underdense tritium plasma channel with a parabolic density profile $n = n_1 + \Delta n(y^2/y_0^2)$, where $n_1 = 0.15n_c$, $\Delta n = 2n_c, y_0 = 50\lambda$, and it is located in $50.8\lambda < x \le 600\lambda, -40\lambda \le y \le 40\lambda$. The simulation box is

a)x.yan@pku.edu.cn.
b)xthe@iapcm.ac.cn.

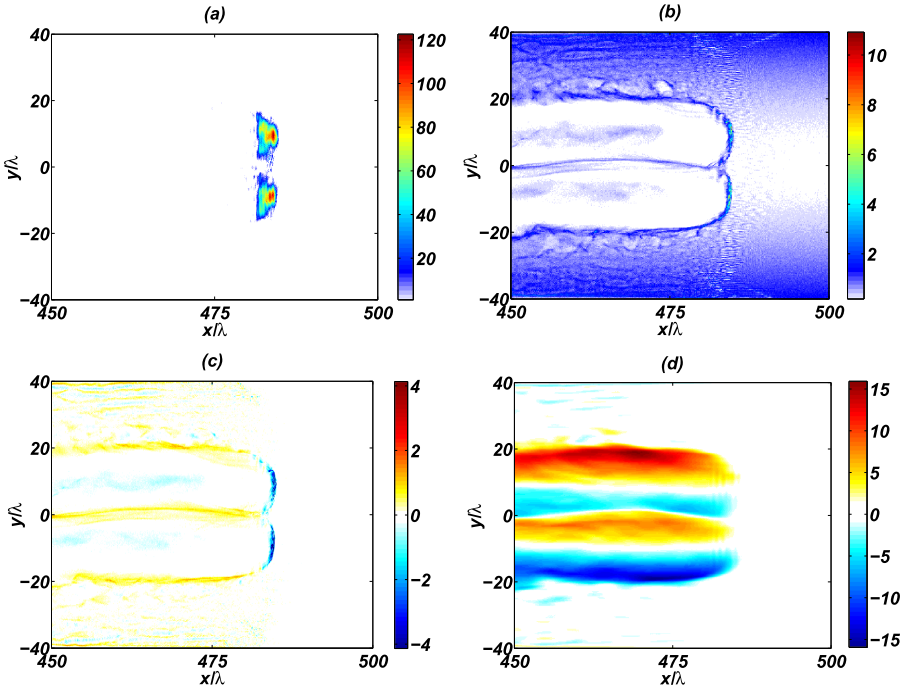

FIG. 1. (a) Square root of the laser intensity $\sqrt{E_y^2+E_z^2}$, normalized by $\mathcal{E}_0$. (b) Electron density normalized by n_c. (c) Current density j_x normalized by en_cc. (d) Spatial distribution of transverse quasistatic field $E_{ys}-B_{zs}$ (in the $\pm y$ directions), normalized by $\mathcal{E}_0$, at $t\sim 500T$.

of size $100\lambda\times 100\lambda$, corresponding to a moving window consisting of 3200×1000 cells, with each cell containing 800 macroparticles for the target and 6 for the underdense channel.

Figs. 1(a) and 1(b) show the square root of the laser intensity and electron density, respectively, at $t\sim 500T$. The transverse size $h=20\,\mu$m of the MLT is smaller than the laser spot size. The incoming laser pulse is split into two by the target. After passing the latter they continue to propagate forward in the preformed backside underdense plasma channel as adjacent twin pulses. The ponderomotive force of the latter expels the local plasma electrons transversely outward, creating two adjacent wakes, or twin wakes, which trap the RPA target protons in them. Fig. 1(c) shows the longitudinal current density j_x at $t\sim 500T$. One can see that there is an intense electron return-current sheet between the two wakes. Since the longitudinal velocity v_x of the trapped protons is near the light speed c, the transverse field experienced by the energetic protons can be written as $\mathcal{E}\hat{e}_y=E_{ys}\hat{e}_y+c^{-1}v_x\hat{e}_xc\times B_{zs}\hat{e}_z\sim(E_{ys}-B_{zs})\hat{e}_y$, where E_{ys} and B_{zs} are the self-generated electrostatic and magnetic fields, respectively. Fig. 1(d) shows the total transverse quasistatic field $\mathcal{E}=E_{ys}-B_{zs}$ normalized by $\mathcal{E}_0=m_e\omega c/e$, where m_e and $-e$ are the electron mass and charge, and ω and c are the laser frequency and light speed, at $t\sim 500T$. One can see that the twin wakes act as a moving potential well for confining, stabilizing, and further accelerating (now the second phase by LWFA) the RPA-protons for a long distance in the target-back-side underdense plasma. In addition, since the MLT electrons also move with the twin wakes, the expelled plasma electrons are prevented from rapidly refilling the back side of the channel, so that the latter can remain open for a long distance. The present acceleration mechanism therefore differs significantly from that of the classical bubble/blowout acceleration schemes.[22,28–30]

B. Guiding the twin wakes in the back-side underdense plasma channel

When the initial laser pulse is split by the MLT, the effective spot size σ_1 of each of the resulting twin light pulses is less than that of the original pulse. Similarly, the divergence angle $\theta_d=\sigma_1/Z_R$ is larger and the Rayleigh length $Z_R=\pi\sigma_1^2/\lambda$ smaller. Thus, without the underdense plasma channel behind the target the laser-plasma interaction distance would be rather limited. However, this undesirable scenario is avoided by the presence of a preformed parabolic density channel. To illustrate this effect, a plasma with the density profile $n=[n_1+\Delta n(y^2/y_0^2)]$ is placed at the back of the target. The dispersion relation for relativistic light waves is $\omega^2=c^2k^2+\omega_p^2/\gamma$, where k and $\omega_p/\gamma^{0.5}$ are the wave number and effective background plasma frequency, respectively, and $\gamma\sim\sqrt{1+a^2}$ is the relativistic factor associated with the electron quiver motion. For an ultra-intense CP laser pulse ($a\gg 1$), the index of refraction is $\eta(y)\sim\left[1-\frac{1}{a(y)n_c}\left(n_1+\Delta n\left(\frac{y^2}{y_0^2}\right)\right)\right]^{1/2}$, so that refractive light guiding (RLG) occurs if $d_y\eta<0$. Light diffraction can be cancelled by RLG if the maximum beam focusing angle is larger than the divergence angle θ_d, or

$$\frac{n_1}{2n_c}\left[\frac{1}{a(\sigma)}-\frac{1}{a(h/2)}\right]+\frac{\Delta n}{n_c}\left[\frac{\sigma^2}{a(\sigma)y_0^2}-\frac{(h/2)^2}{a(h/2)y_0^2}\right]\geq\left(\frac{\lambda}{\pi\sigma_1}\right)^2, \tag{1}$$

where the three terms in the inequality represent relativistic self-focusing guiding, preformed density channel RLG, and light diffraction, respectively. We note that this relation differs considerably from that of the $a\ll 1$ case. For the parameters under consideration, the self-focusing and RLG terms have the values ~0.0021 and 0.013, respectively. The latter

alone is already much larger than the diffraction term, which has the value 0.0041. One can also see that without RLG the proton bunch would diverge. Fig. 1(a) shows the profile of the light field at $t \sim 500T$. We see that RLG by the pre-formed parabolic density channel indeed results in long distance propagation of the twin light pulses and the corresponding twin wakes. In fact, the laser-plasma interaction distance is effectively increased to $\sim 7Z_R$. Moreover, the focusing effect of RLG also doubles the intensity of the twin pulses to $a_1 \sim 2a_0 = 120$, as shown in Fig. 1(a).

C. Scaling law for the highly collimated tens-GeV monoenergetic protons

We now consider the evolution of the pre-accelerated protons in more detail. From Figs. 2(a) and 2(c), one sees that the relativistic protons are confined along the original laser axis and they can propagate a long distance without divergence. It can be seen from Figs. 3(a) and 3(b) that these protons undergo further electrostatic acceleration in the twin-wakes along the original laser axis.

In the present twin wakes regime, the profile can be estimated by assuming that the transverse ponderomotive force of the laser $k_p \nabla a_1^2/\gamma \sim a_1/k_p R$, where R and k_p are the transverse radius and plasma wave number, is roughly balanced by the force of the ion channel $E_r \sim k_p R/2$.[30,31] Equating these two expressions yields $k_p R \sim \sqrt{2a_1}$. Moreover, the twin-wakes radius scales with the twin-pulses laser spot, $k_p R \sim k_p \sigma_1$. Through PIC simulation we have found that a more refined condition is $k_p R \sim k_p \sigma_1 \sim \pi\sqrt{a_1}$. Combining these equations, the maximum quasistatic field is thus given, $\mathcal{E}_{\max}(y)/\mathcal{E}_0 \sim (\pi/2)(a_1 n(y)/n_c)^{1/2}$. As a result, the maximum quasistatic transverse field at the center of the channel reads

$$\mathcal{E}_{\max} \sim (\pi/2)(a_1 n_1/n_c)^{1/2}\mathcal{E}_0. \tag{2}$$

Fig. 1(d) shows that the maximum quasistatic transverse (or focusing) field $\mathcal{E}_{\max}$ induced by the charge separation, and the return current at the center of the channel is about $6\mathcal{E}_0$, agreeing well with the above theoretical scaling, where $a_1 \sim 2a_0 = 120$ is the laser front intensity due to the RLG effect. The angular distribution of the accelerated protons at $t \sim 600T$ is given in Fig. 2(b), which shows that the average emission angle for protons with energy greater than 8 GeV is less than 2°. That is, the output proton beam is well collimated by the transverse quasistatic field.

When the twin-pulses propagate in the underdense plasma, they etch back with v_{etch} due to local pump depletion, since the twin-pulses strongly interact with the front compressed electron layers because their rear parts are in a region of electron void. The laser will be depleted after a distance (pump depletion length), $L_{pd} \sim (c/v_{\text{etch}})c\tau_{\text{FWHM}}$, where $c\tau_{\text{FWHM}}$ is laser pulse duration. Furthermore, the laser pump depletion length can be estimated by equating the laser pulse energy to the energy left behind in the wakefield, $\mathcal{E}^2_{y=\pm h/2} L_{pd} \sim \mathcal{E}_l^2 c\tau_{\text{FWHM}}$, where $\mathcal{E}^2_{y=\pm h/2} \sim \pi(a_1 n_1/n_c)^{1/2}\mathcal{E}_0$ and $\mathcal{E}_l$ are the maximum quasistatic field and laser field of twin-pulses front, respectively. The laser etching velocity is thus $v_{\text{etch}} \sim \pi^2 n_1 c/a_1 n_c$.

The distance that the trapped protons travel until they outrun the twin-wakes (dephasing length) is approximately $L_{dp} \sim l_{\text{inj}} v_p/(v_p - v_f) = l_{\text{inj}} v_p/[v_p - (v_g - v_{\text{etch}})]$, where v_p and $v_f = v_g - v_{\text{etch}}$ are the proton velocity and laser front velocity, v_g and v_{etch} are group velocity and etching velocity of laser pulse, $l_{\text{inj}} \sim \frac{R}{2}$ from the simulation. When v_p and v_g are both near the light speed c, so that $v_{\text{etch}} \gg v_p - v_g$, the proton dephasing length becomes

$$L_{dp} \sim \frac{R}{2}\frac{c}{v_{\text{etch}}} \sim \frac{1}{4\pi^2}\left(\frac{a_1 n_c}{n_1}\right)^{3/2}\lambda. \tag{3}$$

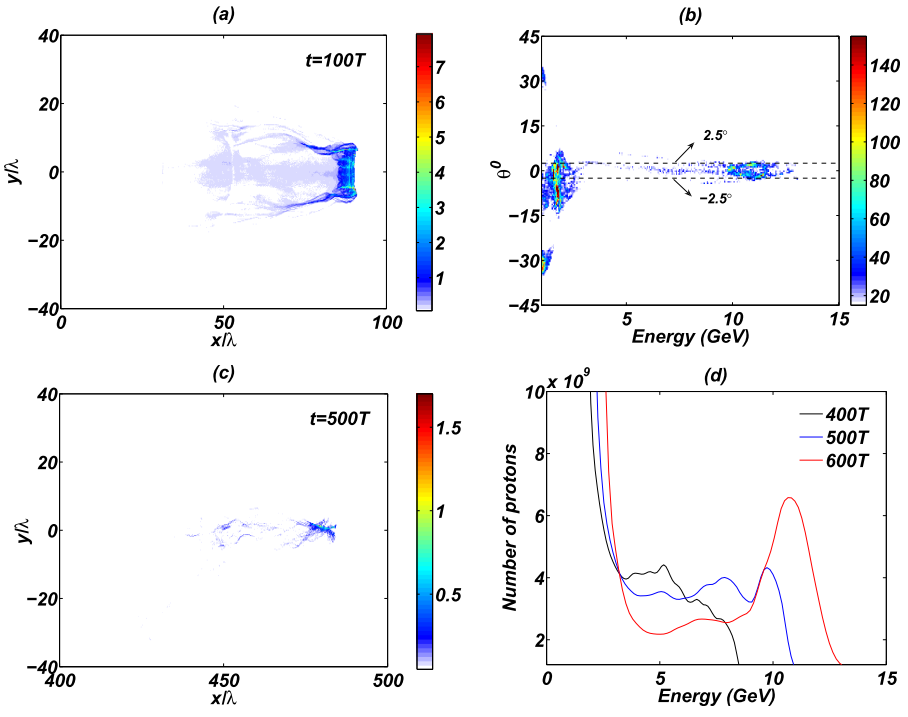

FIG. 2. Density of the accelerated protons in units of n_c at (a) $t \sim 100T$ and (c) $t \sim 500T$. (b) Angular distribution of the protons at $t \sim 600T$. The dashed lines correspond to the divergence angle ±2.5°. (d) Evolution of the proton energy spectrum.

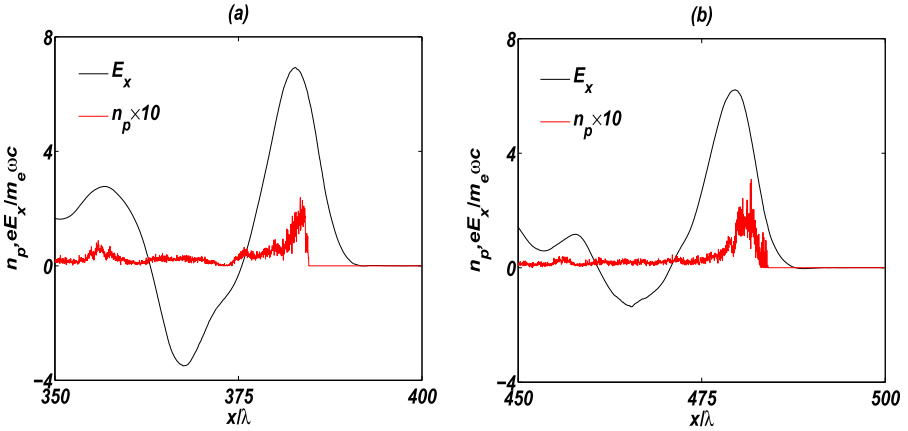

FIG. 3. The proton density n_p and longitudinal electrostatic field $eE_x/m_e\omega c$ along the original laser axis in the twin-wakes regime at (a) $t \sim 400T$ and (b) $t \sim 500T$, respectively.

Figure 4(a) for the temporal evolution of the maximum proton energy shows clearly the two stages, namely, RPA and LWFA, of the acceleration process. In the initial RPA regime, the maximum proton velocity reaches $0.945c$, or 1.93 GeV, at $t \sim 100T$. The pre-accelerated protons then undergo LWFA in the twin wakes until the light pulses are almost depleted at $t \sim 600T$, implying that pump depletion length is about $L_{pd} \simeq 600\,\mu$m. At that time, the trapped proton bunch approaches the front of the twin wakes. That is, the dephasing length L_{dp} is roughly the same as L_{pd}. The latter is also consistent with the theoretical value, as calculated by Eq. (3).

We also see that the maximum proton energy increases rapidly with time until $t \sim 600T$, when saturation occurs. Using the conditions for the stable twin wakes excitation, we can estimate the energy gain of the trapped proton beam by using the above equations,

$$\Delta E = eE_{\mathrm{LW}}L_{dp} \sim (a_1^2 n_c/n_1)m_e c^2/4, \tag{4}$$

where $E_{\mathrm{LW}} \sim (\pi/2)(a_1 n_1/n_c)^{1/2}\mathcal{E}_0$ is the average accelerating field due to the space-charge additive effect at the center of the twin wakes. Fig. 2(d) shows the evolution of energy spectrum. One can see that the latter improves with time and eventually achieves a sharp peak at about 12 GeV, which is highly consistent with the analytical model. Fig. 4(b) shows that the number of protons in the region $|y| \leq 3\lambda$ first decreases and then becomes constant at 1.5×10^{11}, indicating that the transverse spreading effect for the energetic protons is well under control in the back-side channel. Their total energy is above 500 J and the laser conversion efficiency is greater than 10%. The accelerated protons are well compressed in the phase space and the quasi-monoenergetic pulse has a duration of about 30 fs. The proton energy is plotted versus the foil thickness in Fig. 4(c). If the foil

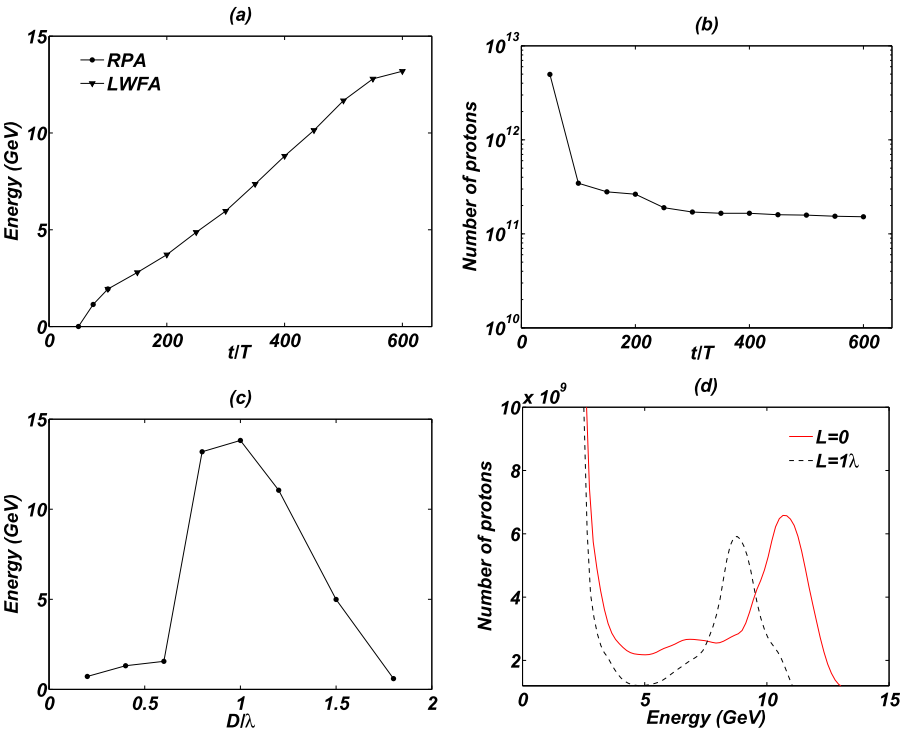

FIG. 4. Evolution of the (a) maximum proton energy, (b) number of protons in the axis region ($|y| \leq 3\lambda$), (c) proton energy versus the foil thickness D, (d) proton energy spectrum at $t = 600T$ with different preplasma density scale length from PIC simulations.

thickness were less than 0.8 μm, the foil protons would not be sufficiently pre-accelerated in the RPA regime and they would not be trapped by the twin wakes. On the other hand, if the foil thickness were greater than 1.2 μm, the dephasing length would be much lowered in the LWFA regime, resulting in sharp decrease of the final proton energies. The optimum proton spectra can be obtained with foil thickness in the range 1.0 − 1.2 μm.

D. Preplasma effect

At present, contrasts at about 10^{12} can be achieved experimentally[32] for amplified spontaneous emission (ASE) pulses at $I = 10^{10}$ W/cm^2. In order to model ASE and prepulse effects, we use a preplasma density profile obtained from hydrodynamic simulations.[33] Typically, the preplasma in the moderately overdense region has a density scale length $L = 1\lambda$. Compared to the $L = 0$ case, more laser energy is depleted in laser-foil interaction stage, so that the pump depletion length is reduced. However, the RPA preaccelerated protons can be still trapped and collimated by the twin wakes. Fig. 4(d) shows that, because of the reduced pump depletion length, the peak proton energy is about 9 GeV, or smaller than that in the case of $L = 0$.

E. Single-wake case

A key issue in the proposed scheme is the formation of a stable proton focusing and collimating twin-wakes structure that moves at a relativistic speed with the target-modulated laser light. When the transverse size of target is too large comparing to the laser spot size, the initial laser pulse can fully interact with the target. The laser is not split into two parts and no twin wakes are formed. Without the transverse confinement in the underdense region, the RPA protons would diverge. This can be seen in the simulation by setting $h = 2\sigma = 40\,\mu$m, with the other laser and plasma parameters the same as in the preceding simulations. Instead of the stable twin wakes (as in Fig. 1(b)) a single wake is now generated by the laser pulse. Due to the defocusing effect of the space-charge field, the RPA protons quickly diverge in the wake, as can be seen in Fig. 5(b) for the emission angle (almost 20°) at $t \sim 600T$. Protons that deviate from the axis region do not experience LWFA. The maximum energy of the accelerated protons is only about 5 GeV, which is considerably lower than that in the stable twin-wakes case (Fig. 2(d)). The quality of the final proton bunch is thus relatively poor in terms of energy gain as well as emission angle.

F. Uniform back-side underdense plasma

The condition (1) for guiding the laser light in the underdense plasma is also important. If the maximum focusing angle is less than the beam divergence angle, RLG of the twin pulses in the density channel cannot occur. To see this, we set $\Delta n = 0$ (uniform plasma behind the target), with the other parameters unchanged. That is, the density-channel guiding effect is removed. For this case in consideration, the relativistic self-focusing term has the value ~0.0021, which is less than the beam diffraction term. It can not prevent the pulses from diffraction and the resulting acceleration process becomes unstable. Fig. 5(c) shows the density distribution of electrons in this case. We see that although a twin-wakes structure is still formed, but it does not survive for a long time. Only a fraction of the RPA protons is further accelerated in the much reduced distance than that in the preformed channel. In addition, the average divergence angle is considerably larger, namely 14°, as shown in Fig. 5(d).

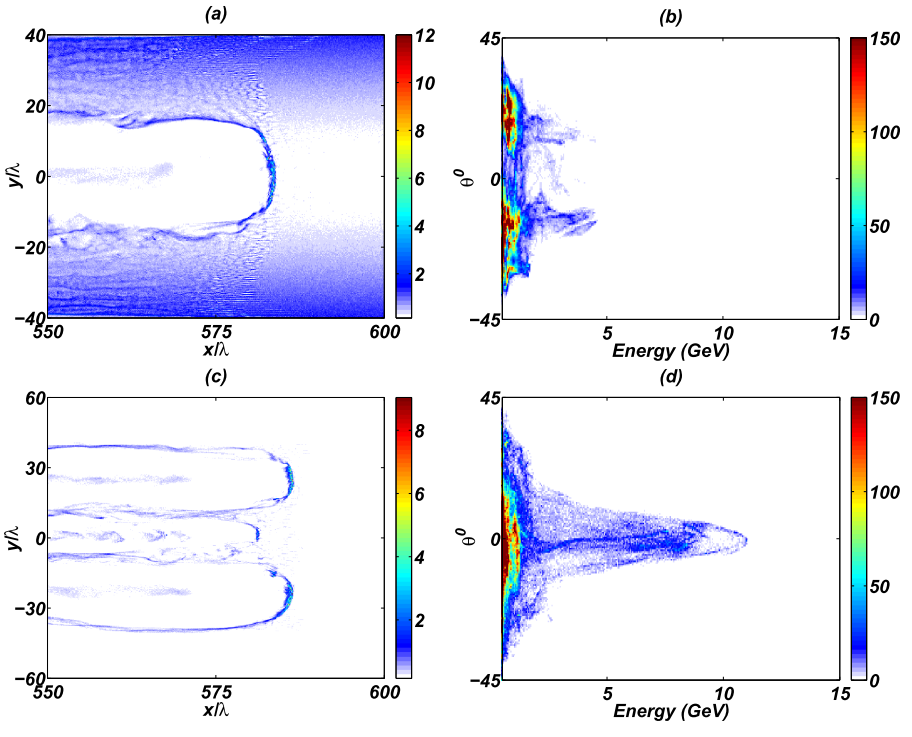

FIG. 5. Electron density at $t \sim 600T$ for the (a) single-wake (when the condition $h \leq \sigma$ is not satisfied) and (c) without guiding channel. The corresponding angular distributions of the protons are shown in (b) and (d), respectively.

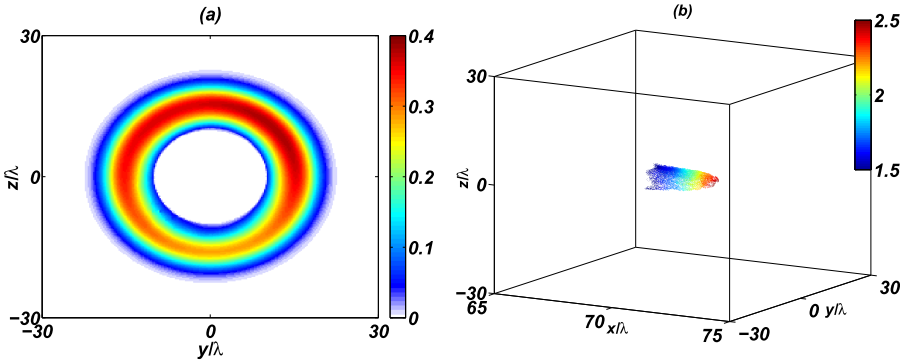

FIG. 6. (a) (z, y) section of the square root of the laser front intensity $\sqrt{E_y^2 + E_z^2}$, normalized by $\mathcal{E}_0$; (b) energy density of the accelerated protons (in units of GeV), at $t = 80T$.

III. 3D SIMULATION

To ensure that the obtained results are not 2D artifacts, we have also carried out 3D simulations. Because of limitation in the computing resources, we consider a narrow simulation box, namely, $60 \times 60 \times 100\lambda^3$. A circular target with density of $25n_c$ and radius $r = 3\lambda$ is used, while its initial position is moved to $x = 10\lambda$. The underdense plasma channel at the backside of the target, with density profile $n = 0.25n_c + 1.25n_c(r^2/r_0^2)$ is located in $11\lambda \le x \le 100\lambda$, $-10\lambda \le y \le 10\lambda$, $-10\lambda \le z \le 10\lambda$, where $r_0 = 20\lambda$. The laser spot size and duration are also reduced to be 8λ and $12T$, respectively. Fig. 6(a) displays the transverse intensity profile of laser front at $t = 80T$, where the center part of laser pulse is depleted. It evolves into a torus in 3D case instead of twin wakes. The trapped protons then undergo further acceleration as well as collimation in the torus, indicating the dynamical process of the accelerated protons is very similar to the 2D case. Fig. 6(b) shows that the accelerated protons are tightly compressed to a spotsize of less than 2.5 μm, and the maximum energy of protons reaches about 2.5 GeV at $t = 80\,T$.

IV. CONCLUSION

In conclusion, an efficient laser-driven proton acceleration scheme using a MLT with a preformed parabolic underdense channel is proposed. The laser pulse drives the target protons by RPA and is split by the MLT into two parts, generating behind them a twin-wakes structure in the channel. The pre-accelerated RPA target protons are efficiently collimated and further accelerated by LWFA in the twin wakes. With this scheme, both light diffraction and proton defocusing are avoided, making long-distance acceleration possible. The conditions and characteristics of proton acceleration from the PIC simulations agree well with that from the analytical estimates. It is shown that ultrashort (30 fs) highly collimated monoenergetic proton bunches with a peak energy of >10 GeV can be produced with a 60 fs CP laser pulse of intensity about 10^{22} W/cm^2. Such a short and collimated proton pulse can be used to excite a plasma wakefield that can in turn accelerate the plasma electrons.[34]

ACKNOWLEDGMENTS

This work is supported by the National Natural Science Foundation of China (Grant Nos. 10835003, 10935003, 10974022, 11175026, 11175029, 11272026), and the National Basic Research Program of China (Grant Nos. 2008CB717806, 2012CB801111).

[1]S. V. Bulanov, T. Zh. Esirkepov, V. S. Khoroshkov, A. V. Kuznetsov, and F. Pegoraro, Phys. Lett. A **299**, 240 (2002).
[2]M. Roth, T. E. Cowan, M. H. Key, S. P. Hatchett, C. Brown, W. Fountain, J. Johnson, D. M. Pennington, R. A. Snavely, S. C. Wilks, K. Yasuike, H. Ruhl, F. Pegoraro, S. V. Bulanov, E. M. Campbell, M. D. Perry, and H. Powell, Phys. Rev. Lett. **86**, 436 (2001).
[3]M. Borghesi, A. Schiavi, D. H. Campbell, M. G. Haines, O. Willi, A. J. Mackinnon, P. Patel, M. Galimberti, and L. A. Gizzi, Rev. Sci. Instrum. **74**, 1688 (2003).
[4]C. K. Li, F. H. Séguin, J. A. Frenje, M. Rosenberg, R. D. Petrasso, P. A. Amendt, J. A. Koch, O. L. Landen, H. S. Park, H. F. Robey, R. P. J. Town, A. Casner, F. Philippe, R. Betti, J. P. Knauer, D. D. Meyerhofer, C. A. Back, J. D. Kilkenny, and A. Nikroo, Science **327**, 1231 (2010).
[5]D. H. H. Hoffmann, A. Blazevic, P. Ni, O. Rosmej, M. Roth, N. A. Tahir, A. Tauschwitz, S. Udrea, D. Varentsov, K. Weyrich, and Y. Maron, Laser Part. Beams **23**, 47–53 (2005), available at http://journals.cambridge.org/action/displayAbstract?fromPage=online&aid=310085.
[6]P. M. Nilson, L. Willingale, M. C. Kaluza, C. Kamperidis, S. Minardi, M. S. Wei, P. Fernandes, M. Notley, S. Bandyopadhyay, M. Sherlock, R. J. Kingham, M. Tatarakis, Z. Najmudin, W. Rozmus, R. G. Evans, M. G. Haines, A. E. Dangor, and K. Krushelnick, Phys. Rev. Lett. **97**, 255001 (2006).
[7]C. K. Li, F. H. Séguin, J. A. Frenje, J. R. Rygg, R. D. Petrasso, R. P. J. Town, O. L. Landen, J. P. Knauer, and V. A. Smalyuk, Phys. Rev. Lett. **99**, 055001 (2007).
[8]Q. L. Dong, S. J. Wang, Q. M. Lu, C. Huang, D. W. Yuan, X. Liu, X. X. Lin, Y. T. Li, H. G. Wei, J. Y. Zhong, J. R. Shi, S. E. Jiang, Y. K. Ding, B. B. Jiang, K. Du, X. T. He, M. Y. Yu, C. S. Liu, S. Wang, Y. J. Tang, J. Q. Zhu, G. Zhao, Z. M. Sheng, and J. Zhang, Phys. Rev. Lett. **108**, 215001 (2012).
[9]M. Borghesi, J. Fuchs, S. V. Bulanov, A. J. Mackinnon, P. Patel, and M. Roth, Fusion Sci. Technol. **49**, 412 (2006), available at http://www.new.ans.org/pubs/journals/fst/a_1159.
[10]G. A. Mourou, T. Tajima, and S. V. Bulanov, Rev. Mod. Phys. **78**, 309–371 (2006).
[11]X. Q. Yan, C. Lin, Z. M. Sheng, Z. Y. Guo, B. C. Liu, Y. R. Lu, J. X. Fang, and J. E. Chen, Phys. Rev. Lett. **100**, 135003 (2008).
[12]O. Klimo, J. Psikal, J. Limpouch, and V. T. Tikhonchuk, Phys. Rev. ST Accel. Beams **11**, 031301 (2008).
[13]A. P. L. Robinson, M. Zepf, S. Kar, R. G. Evans, and C. Bellei, New J. Phys. **10**, 013021 (2008).
[14]X. Q. Yan, H. C. Wu, Z. M. Sheng, J. E. Chen, and J. Meyer-ter-Vehn, Phys. Rev. Lett. **103**, 135001 (2009).
[15]B. Qiao, M. Zepf, M. Borghesi, and M. Geissler, Phys. Rev. Lett. **102**, 145002 (2009).
[16]T. Esirkepov, M. Borghesi, S. V. Bulanov, G. Mourou, and T. Tajima, Phys. Rev. Lett. **92**, 175003 (2004).
[17]Z. M. Zhang, X. T. He, Z. M. Sheng, and M. Y. Yu, Phys. Plasmas **17**, 043110 (2010).
[18]B. F. Shen, X. Zhang, Z. M. Sheng, M. Y. Yu, and J. Cary, Phys. Rev. ST Accel. Beams **12**, 121301 (2009).
[19]L. L. Yu, H. Xu, W. M. Wang, Z. M. Sheng, B. F. Shen, W. Yu, and J. Zhang, New J. Phys. **12**, 045021 (2010).

[20]F. L. Zheng, H. Y. Wang, X. Q. Yan, T. Tajima, M. Y. Yu, and X. T. He, Phys. Plasmas **19**, 023111 (2012).
[21]F. L. Zheng, S. Z. Wu, C. T. Zhou, H. Y. Wang, X. Q. Yan and X. T. He, Europhys. Lett. **95**, 55005 (2011).
[22]T. Tajima and J. M. Dawson, Phys. Rev. Lett. **43**, 267 (1979).
[23]B. Qiao, M. Zepf, M. Borghesi, B. Dromey, M. Geissler, A. Karmakar, and P. Gibbon, Phys. Rev. Lett. **105**, 155002 (2010).
[24]S. V. Bulanov, E. Yu. Echkina, T. Zh. Esirkepov, I. N. Inovenkov, M. Kando, F. Pegoraro, and G. Korn, Phys. Rev. Lett. **104**, 135003 (2010).
[25]X. M. Zhang, B. F. Shen, L. L. Ji, F. C. Wang, M. Wen, W. P. Wang, J. C. Xu, and Y. H. Yu, Phys. Plasmas **17**, 123102 (2010).
[26]T. Sokollik, T. Paasch-Colberg, K. Gorling, U. Eichmann, M. Schnürer, S. Steinke, P. V. Nickles, A. Andreev, and W. Sandner, New J. Phys **12**, 11301 (2010), available at http://iopscience.iop.org/1367-2630/12/11/113013/fulltext/.
[27]Z. M. Sheng, K. Mima, Y. Sentoku, K. Nishihara, and J. Zhang, Phys. Plasmas **9**, 3147 (2002).
[28]A. Pukhov and J. Meyer-ter-Vehn, Appl. Phys. B **74**, 355 (2002).
[29]W. P. Leemans, B. Nagler, A. J. Gonsalves, C. Toth, K. Nakamura, C. G. R. Geddes, E. Esarey, C. Schroeder, and S. M. Hooker, Nature Phys. **2**, 696 (2006).
[30]W. Lu, C. Huang, M. Zhou, and M. Tzoufras, Phys. Plasmas **13**, 056709 (2006).
[31]W. Lu, M. Tzoufras, C. Joshi, F. S. Tsung, W. B. Mori, J. Vieira, R. A. Fonseca, and L. O. Silva, Phys. Rev. ST Accel. Beams **10**, 061301 (2007).
[32]A. Henig, D. Kiefer, K. Markey, D. C. Gautier, K. A. Flippo, S. Letzring, R. P. Johnson, T. Shimada, L. Yin, B. J. Albright, K. J. Bowers, J. C. Fernández, S. G. Rykovanov, H.-C. Wu, M. Zepf, D. Jung, V. Kh. Liechtenstein, J. Schreiber, D. Habs, and B. M. Hegelich, Phys. Rev. Lett. **103**, 045002 (2009).
[33]H. B. Cai, K. Mima, A. Sunahara, T. Johzaki, H. Nagatomo, S. P. Zhu, and X. T. He, Phys. Plasmas **17**, 023106 (2010).
[34]A. Caldwell, K. Lotov, A. Pukhov, and F. Simon, Nature Phys. **5**, 363 (2009).